

## Turbulence characteristics inside a turbulent spot in plane Poiseuille flow

By D.S. Henningson<sup>1</sup>, J. Kim<sup>2</sup>, & P. H. Alfredsson<sup>3</sup>

### 1. Introduction

In wall-bounded shear flows the transition to turbulence through localized disturbances goes through a pattern starting with a development of shear layers. The localized normal velocity fluctuations induce normal vorticity through the lift-up effect (Gustavsson, 1978; Henningson, 1988; Landahl, 1975). These shear layers become unstable to secondary disturbances (Breuer, 1988), and if the amplitudes of the disturbances are large enough, a turbulent spot develops (Chambers & Thomas, 1983). The spot develops in approximately a self-similar manner with an average spreading angle of about 10° for most wall-bounded shear flows (Riley & Gad-el-Hak, 1985). In plane Poiseuille flow spanwise wingtips of a spot consist of large-amplitude wave packets that breakdown as they propagate into the spot. The breakdown of the wave packets has been observed both in experiments (Henningson & Alfredsson, 1987) and in a numerical simulation (Henningson et al., 1987). The experiments have shown that the wave packets consist of the least stable Tollmien-Schlichting (T-S) mode. Analysis of the simulation data using kinematic wave theory has also shown that the wave breakdown is closely related to the spot spreading (Henningson, 1988).

Investigations of the spot in boundary layers has shown that the turbulent part of the spot is very similar to fully-developed boundary layer. Wygnanski et al. (1976) showed that the mean profile at the center-symmetry plane has a logarithmic region and Johansson et al. (1987) showed that both the higher-order statistics and flow structures in the spot were the same as in the corresponding fully-developed flow. The aim of the present investigation is to study in what respects the turbulence inside the Poiseuille spot is similar to fully developed turbulent channel flow. The numerically simulated spot (Henningson et al. 1987) will be used in the present investigation, where the characteristics inside the spot will be compared to those of the wave packet in the wingtip area. A recent experimental investigation of the velocity field associated with the Poiseuille spot by Klingmann et al. (1988) will be used for comparison.

### 2. Eduction of Mean Velocity

<sup>1</sup> Massachusetts Institute of Technology

<sup>2</sup> NASA Ames Research Center

<sup>3</sup> Royal Institute of Technology

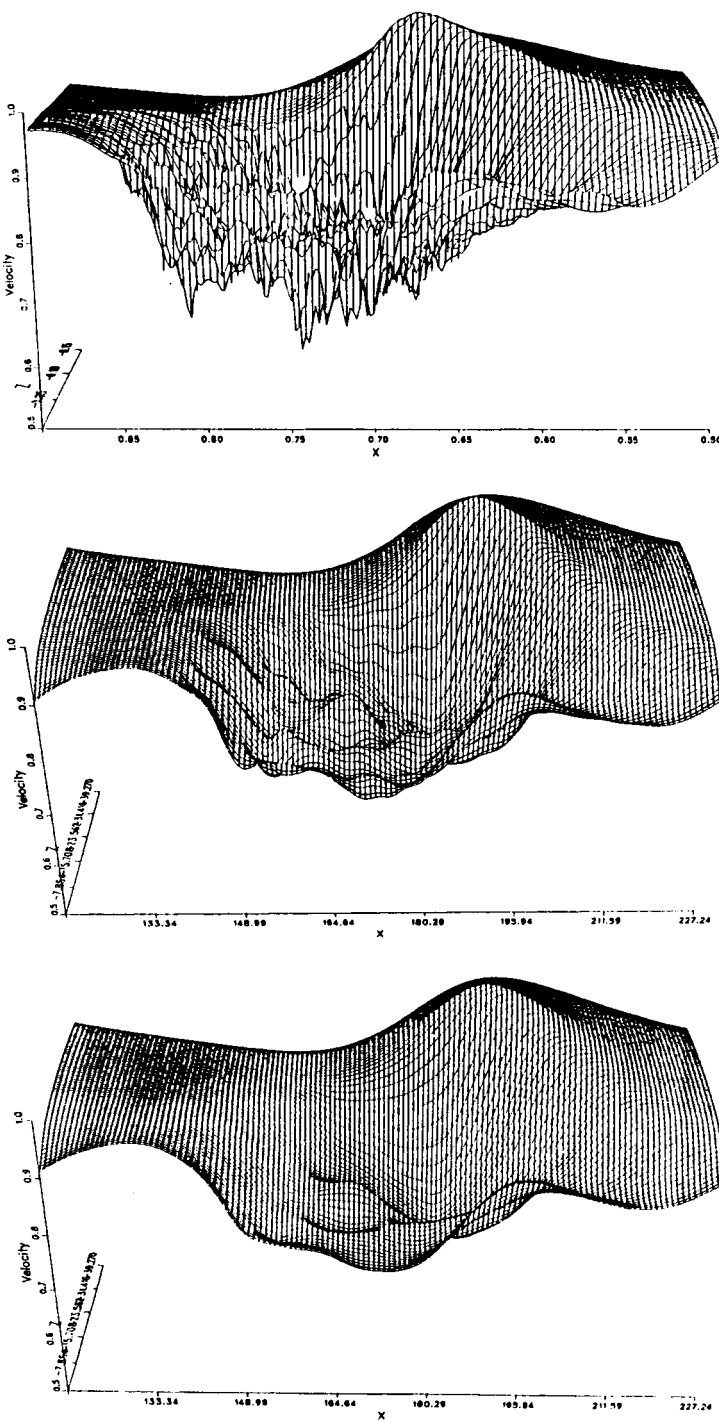


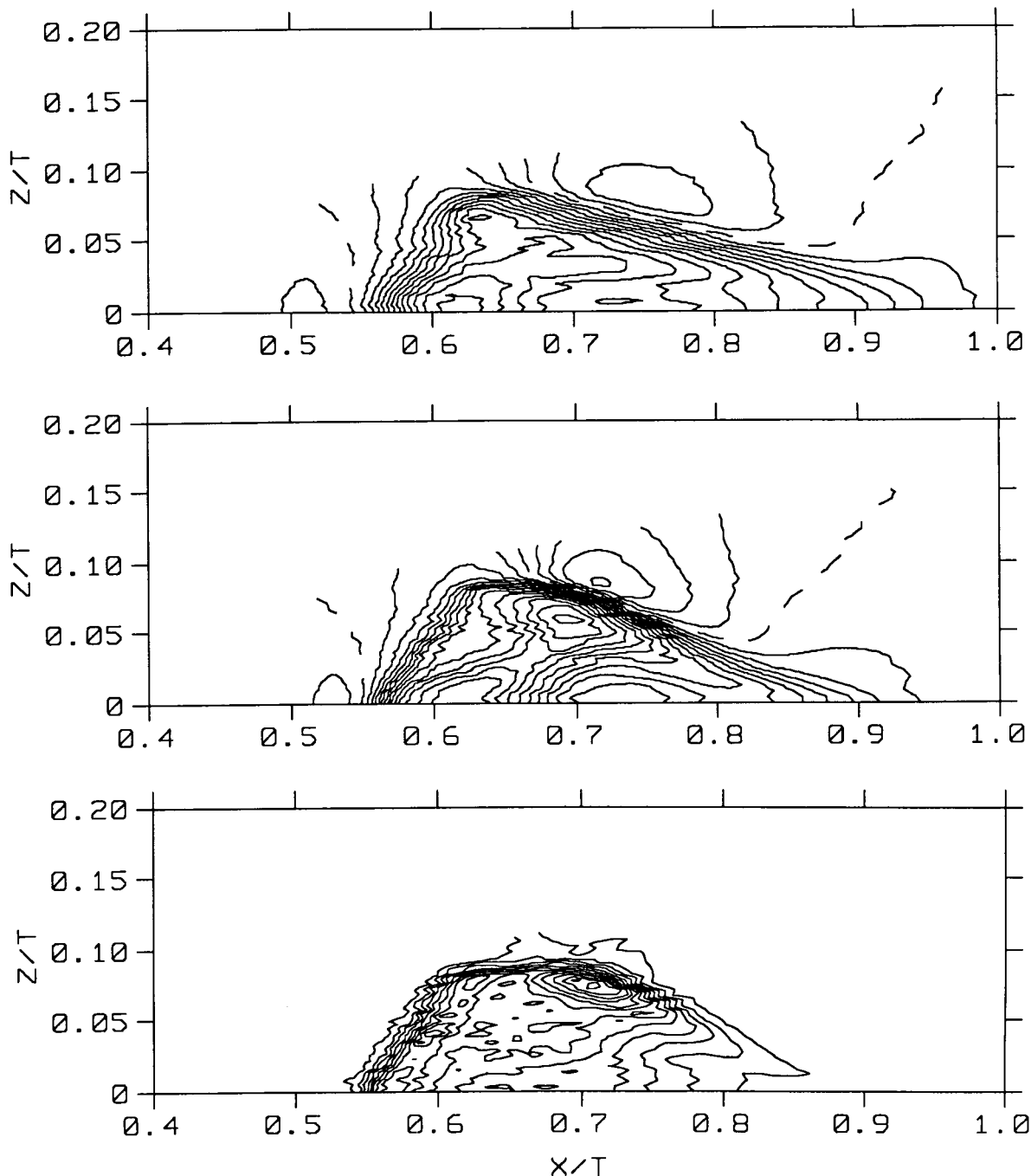
FIGURE 1. Surfaces of streamwise mean velocity at the centerline, a) conical averaging, b) and c) Gaussian filters with different filter widths at  $t=258$ . Note that only half the spot is shown.

The numerical simulation of a turbulent spot in plane channel was performed at Reynolds number of 1500 based on the centerline velocity ( $U_c$ ) and the channel half-width ( $h$ ). The reader is referred to Henningson et al. (1987) for details regarding the simulation. Because of its enormous cost of computation, no attempt was made to run several cases to obtain ensemble-averaged statistics. In order to compare the simulation results from this single realization to the ensemble-averaged results obtained from experiments, a mean velocity has to be defined. Analysis of the fluctuating components also requires a well defined mean. Since the spot is approximately self similar, a conical averaging procedure was tried first. One hundred and twenty velocity fields between  $t = 222$  and  $t = 258$  were interpolated into a conical coordinate system and added together. The horizontal conical coordinates were defined as  $\xi = x/t$  and  $\zeta = z/t$ . The mean velocity obtained from this procedure was not smooth enough to be regarded as a mean as shown in Fig. 1a, where the surface representing the streamwise velocity at the centerline ( $y = 0$ ) is plotted. The conical average of the normal velocity revealed more small-scale structures that survived the averaging process. Spatial averaging was also tried using Gaussian filters. Figures 1b and 1c show the results obtained by using two different filter widths. The Gaussian-filtered velocity field shown in Fig. 1c was chosen to represent the mean because the velocity fluctuations from the other two averages were judged to be too large in the turbulent area of the spot. The problem with a fairly wide Gaussian-filter function (in physical space) is that sharp gradients in the mean flow are smoothed out as well when the small scales are removed. This was observed at the transition region where sharp gradients exist.

The ensemble-averaged results from Klingmann et al. (1988) and those obtained from the procedure mentioned above are shown in Figs. 2 and 3, respectively. Agreement between the two results are remarkable: the sharp transition region with the dip in the velocity, the arrow head front part of the disturbance, and the speed-up of the laminar fluid around the spot. One may conclude from this comparison that the spatial average can reasonably well represent the true ensemble average. The spanwise mean velocity at the centerline is shown in Fig. 3c. Most of the fluid inside the spot can be seen to move outward while the laminar fluid in the front and back of the spot is directed towards the spanwise symmetry line,  $z = 0$ .

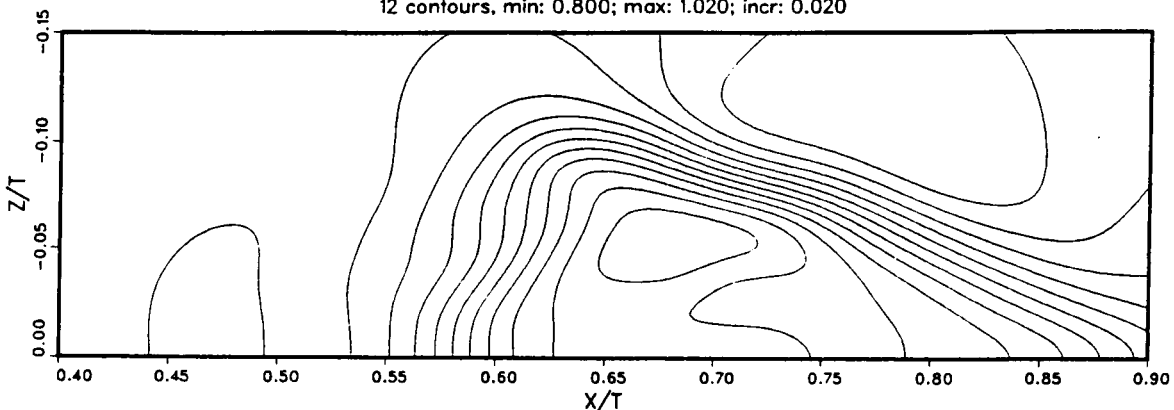
The fluctuating components can be defined as the full simulated velocities with the spatially averaged mean subtracted. Fig. 4 shows contours of streamwise and normal components. In Fig. 4a, we notice an artificial oblique structure at the spanwise wingtip of the spot, resulting from too much smoothing in the sharp gradient between the laminar and turbulent part. The streamwise fluctuating component closer to the wall is shown in Fig. 4b. The long streaky structure typical of near-wall turbulent flows can be seen inside the spot. The wingtip wave packet is discernible at this position, but it can be more clearly seen in the normal velocity at the centerline as shown in Fig. 4c.

The rms fluctuations are also computed from the fluctuating components. Contours of the rms fluctuation of streamwise velocity at the centerline are shown in

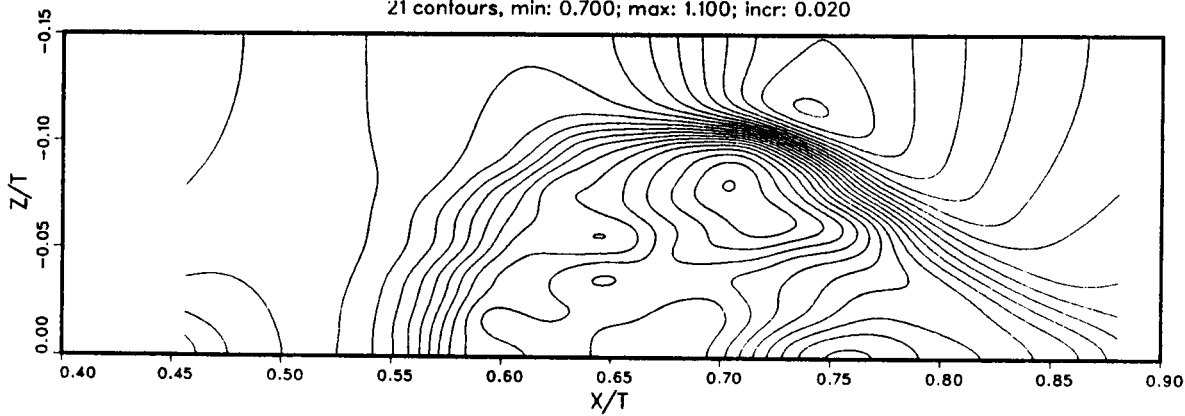


at the centerline (in conical coordinates), a) mean velocity measured at  $x = 100$ , b) mean velocity measured at  $x = 200$ , c) rms velocity measured at  $x = 200$ . Contour spacing is 0.02 in a) and b) and 0.01 in c).

12 contours, min: 0.800; max: 1.020; incr: 0.020



21 contours, min: 0.700; max: 1.100; incr: 0.020



9 contours, min: -0.100; max: 0.060; incr: 0.020

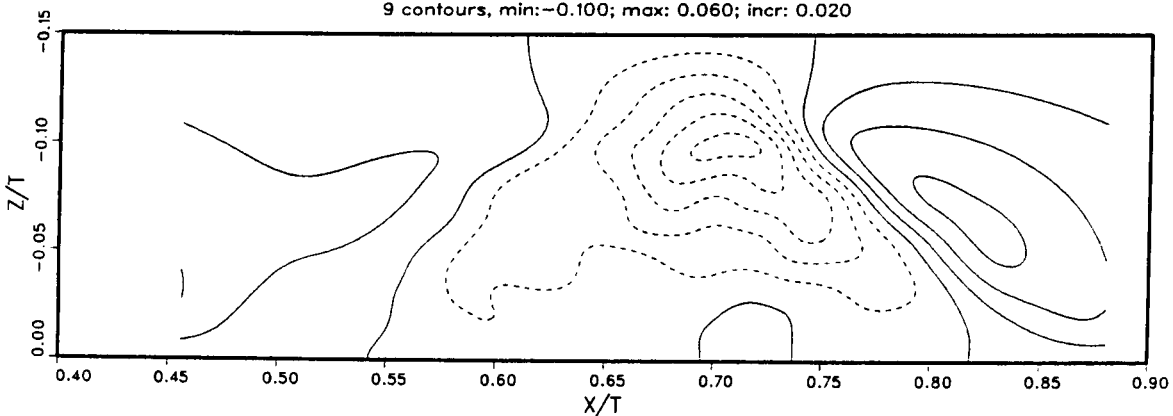
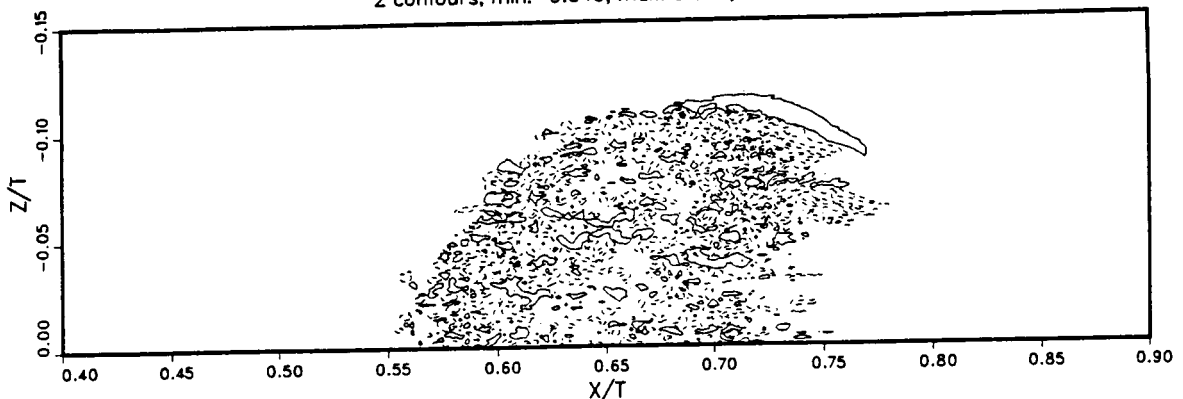
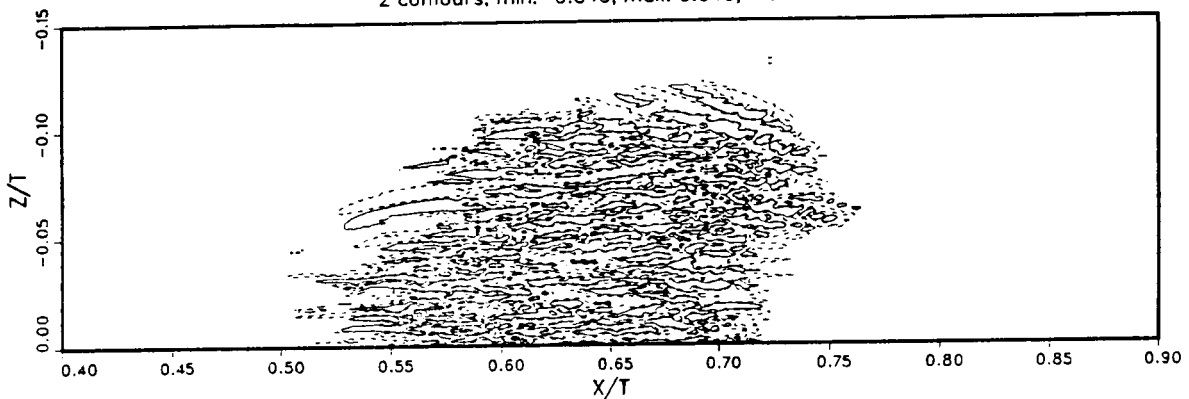


**FIGURE 3.** Contours of mean Gaussian filtered velocity at centerline, a) streamwise velocity for  $t = 138$ , b) streamwise velocity for  $t = 258$ , c) spanwise velocity for  $t = 258$ .

2 contours, min: -0.040; max: 0.040; incr: 0.080



2 contours, min: -0.040; max: 0.040; incr: 0.080



2 contours, min: -0.010; max: 0.010; incr: 0.020

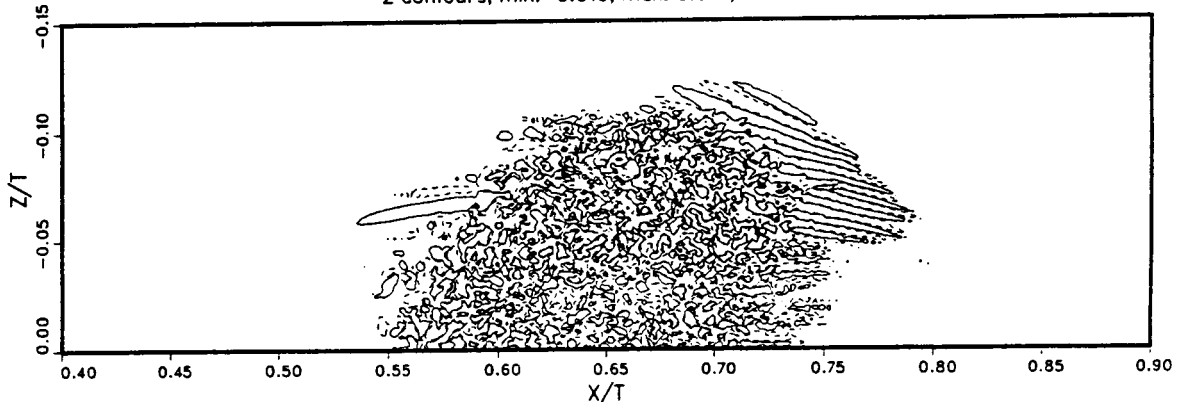


FIGURE 4. Contours of disturbance velocities for  $t = 258$ , a) streamwise velocity at  $y = 0$ , b) streamwise velocity at  $y = -0.83$ , c) normal velocity at  $y = 0$ . Dashed lines in this and following figures indicate negative contour levels unless stated otherwise.

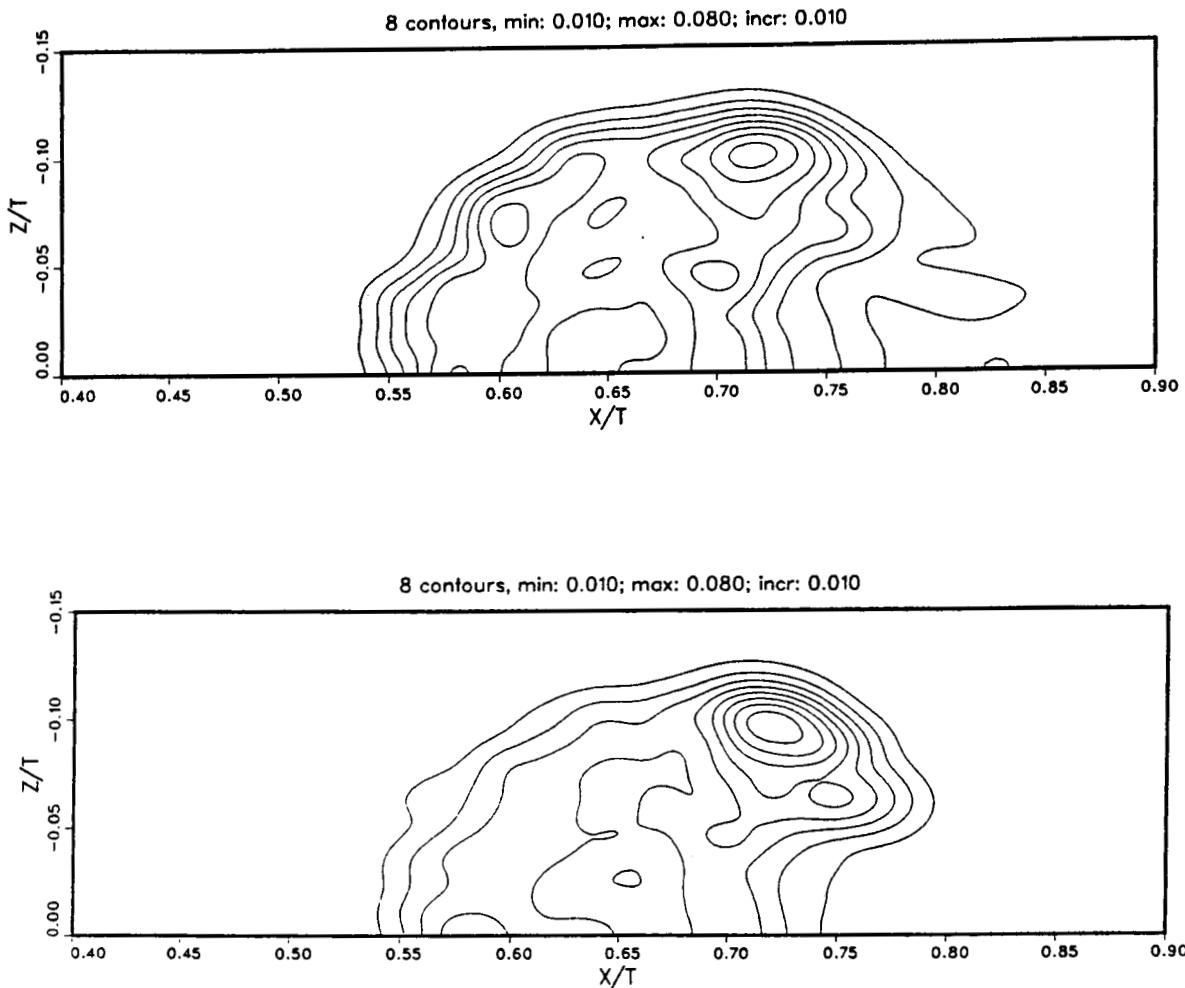


FIGURE 5. Contours of rms velocities for  $t = 258$  at  $y = 0$ , a) streamwise and b) normal velocities.

Fig. 5a. It increases substantially high inside the turbulent part. The corresponding rms fluctuation obtained from experiments by Klingmann et al. is shown in Fig. 2c. They are in good agreement with each other, including the small peak in the wingtip region. This indicates that the peak is not due to the excess disturbance velocity induced by the Gaussian smoothing of the sharp transition gradient. The rms fluctuation of normal velocity at the centerline is shown in Fig. 5b. It is also substantially larger in the turbulent area, but it rises to twice that value in the spanwise wave region. This is a consequence of the high amplitude T-S waves present at the wingtip.

### 3. Comparison with fully-developed turbulent channel flow

In order to compare turbulence characteristics inside the spot with those in fully developed channel flow turbulence, one would like to scale the flow variables with

10 levels, spacing: 0.002 starting at 0.036

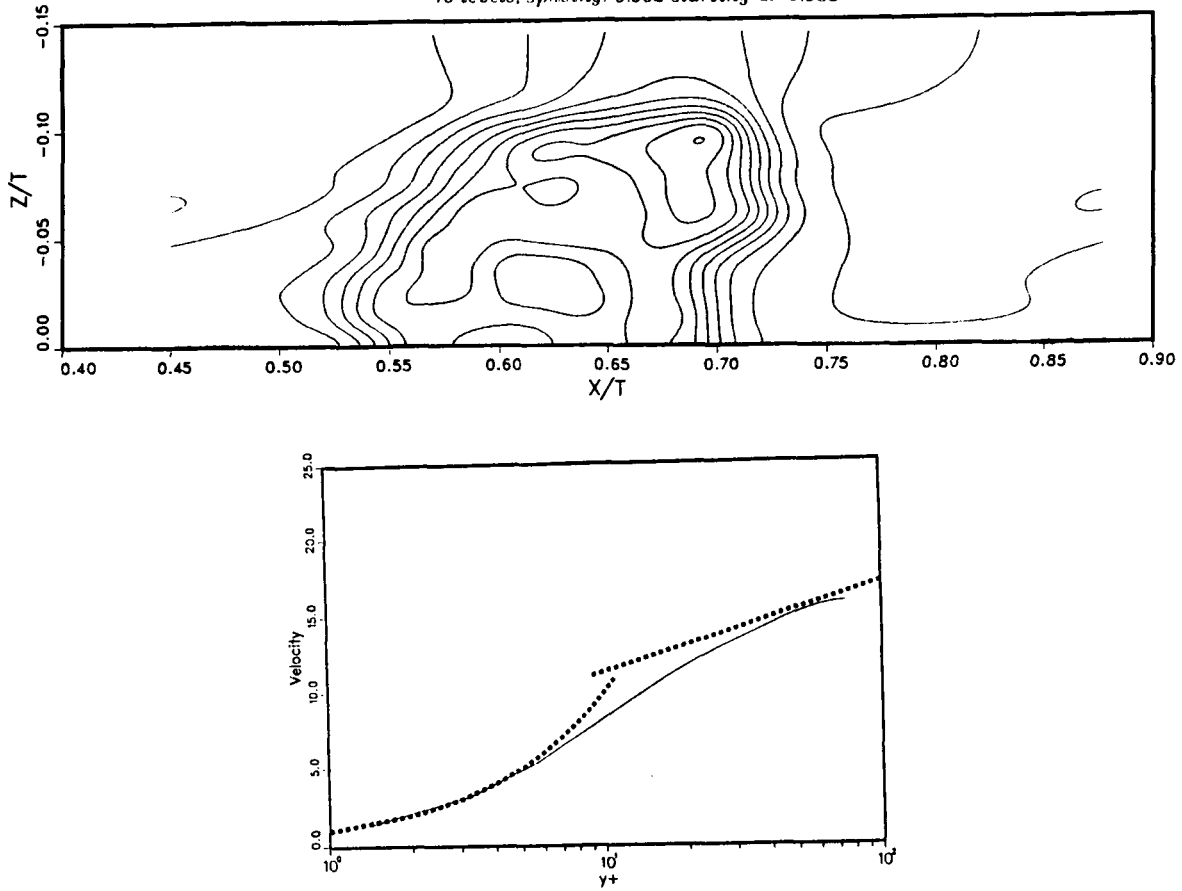


FIGURE 6. a) Contours of  $u_r$  at lower channel wall, b) mean velocity in the lower channel half averaged over the turbulent area compared with the law of the wall and the log-law. Dashed curves are  $u^+ = y^+$  and  $u^+ = 2.5 \ln y^+ + 5.5$ .

the inner-wall scaling, i.e., with the friction velocity  $u_r^* = \sqrt{\nu dU/dy}|_{wall}$  and the kinematic viscosity  $\nu$ . Contours of  $u_r = u_r^*/U_{CL}$  are shown in Fig. 6a. A mean value of  $u_r$  inside the spot was obtained by averaging it in the area  $0.58 < \xi < 0.70$  and  $-0.08 < \zeta < 0.0$  to yield about 0.05. (The above designated area will in the following be referred to as the turbulent area). The  $y$ -dependence of the mean streamwise velocity in the turbulent area is shown in Fig. 6b. The dotted curve is  $u^+ = y^+$  and the line  $u^+ = 2.5 \ln(y^+) + 5.5$ , where the superscript + denotes a quantity scaled by the inner-wall scaling. The log-region is very small since the Reynolds number is low ( $Re_r = u_r h / \nu \approx 70$ ). Considering the low Reynolds number the shape is in good agreement with other simulation and experimental results (Kim et al., 1987). The  $y$ -dependence of the rms values of three velocity components averaged over the turbulent area are shown in Fig. 7a. They are in good agreement with those corresponding to the fully-developed turbulent channel flow, except that the peak in the streamwise velocity close to the wall appears to

be a bit low. To contrast the findings in the turbulent area, a wave area is defined as  $0.70 < \xi < 0.74$  and  $-0.12 < \zeta < -0.08$ . The  $y$ -dependence of the rms values in the wave area is shown in Fig. 7b. All of the fluctuating components are larger in the wave area, and the normal velocity has a different shape, which is somewhat similar to the mode shape of the least stable T-S wave. The Reynolds shear stress both in the turbulent and the wave area is shown in Fig. 7c. In the turbulent area it shows the behavior expected from a fully developed channel flow; in the wave area it is substantially higher, indicating higher turbulence production.

Another characteristic of wall-bounded turbulent shear flows is the sharp shear-layer structures found in the near-wall region. In order to examine the structure of the shear layers, the VISA (Variable-Time Space-Average) technique was used to detect them. This technique has been used by Kim (1985) and Johansson, Alfredsson & Kim (1987) to detect the shear layers in fully-developed turbulent channel flow. Islands of high variance of streamwise velocity were identified for a given flow field, and an ensemble average was obtained by aligning the maximum local variance in the islands for every individual event detected. The results obtained from this procedure is given in Figs. 8 and 9. They appear to be in good agreement with those obtained from the full turbulent simulation. Figures 8a and 8b show the typical inclined shear-layer structure associated with the lift-up of low speed fluid in the downstream and the downward sweep in the upstream. The spanwise structure of the shear layer is shown in Fig. 8c. The spanwise distance between the outer loops is slightly above 100 viscous units, indicating that the average spacing between the low- and high-speed streaks are captured correctly (Kim et al., 1987). The ensemble average of the shear-layer structure in the wave area shows a similar behavior in the normal plane (Fig. 9a), but the horizontal structure clearly reflects the wave-like characteristics (Fig. 9b). The oblique character of the waves can be seen, and more importantly a structure of peaks and valleys in the cross wave direction. This is typical of the secondary breakdown seen in vibrating-ribbon experiments, (Klebanoff et al., 1962; Nishioka et al., 1976). This supports the idea that the secondary instability is responsible for the breakdown of the large-amplitude waves and the subsequent rapid transition to turbulence.

#### 4. Summary and discussion

Using a horizontal Gaussian-filter function a mean and fluctuating components were computed from instantaneous velocity fields obtained from a single realization. The streamwise component of the mean was in good agreement with the ensemble-averaged velocity field obtained from the experiments by Klingmann et al. (1988). The contours of streamwise rms fluctuation also showed a good agreement between the experimental and simulated results.

In the turbulent part of the spot the velocity field was very similar to that of fully-developed turbulent channel flow. The mean velocity and the rms fluctuations as well as the Reynolds shear-stress profiles all showed good agreements. The shear-layer structure obtained from the VISA technique also revealed similar behavior, indicating that the turbulence inside the spot behaves as if it were a fully-developed turbulent channel flow.

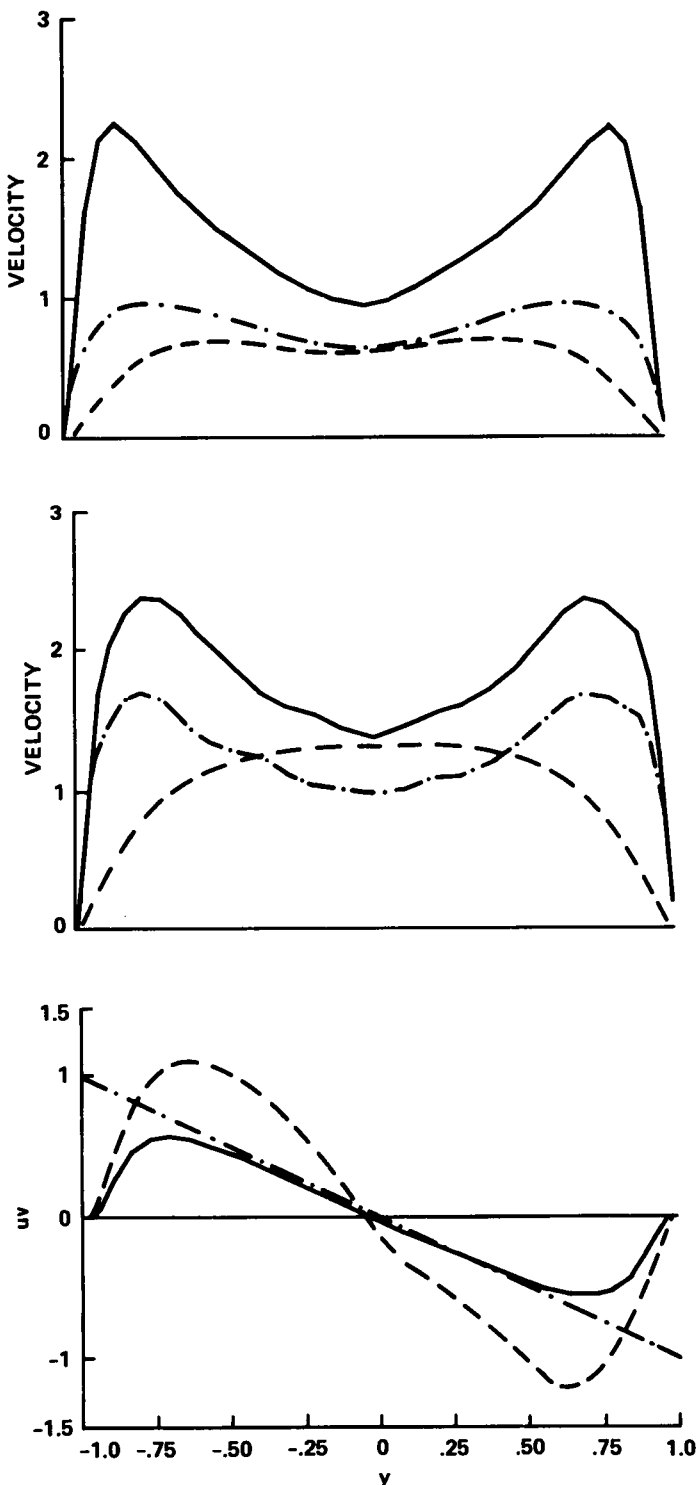
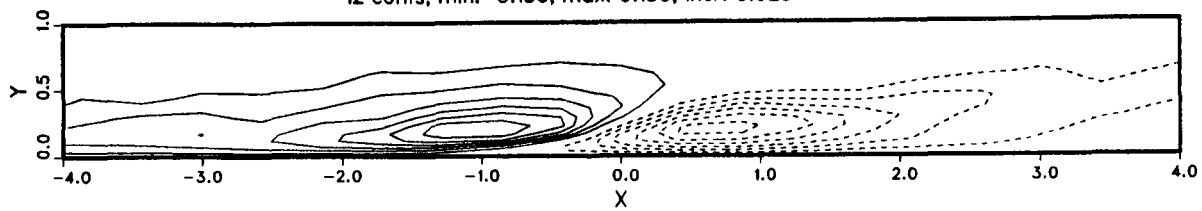
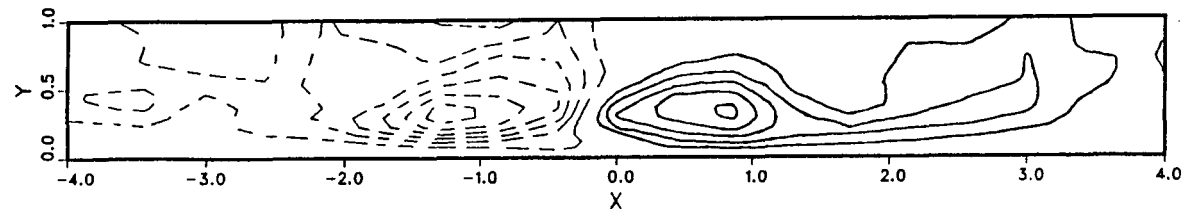


FIGURE 7. a) Rms velocities averaged over the turbulent part, b) rms velocities averaged over the wave area (rms velocities are scaled with mean  $u_r^*$  from the turbulent area: —,  $u_{rms}$ ; ---,  $v_{rms}$ ; ·····,  $w_{rms}$ . c) —, Re却ndols shear stress in turbulent area; ---, wave area; ·····,  $uv = -y$ .

12 conts, min: -0.150; max: 0.150; incr: 0.025



11 conts, min: -0.030; max: 0.025; incr: 0.005



12 conts, min: -0.150; max: 0.150; incr: 0.025

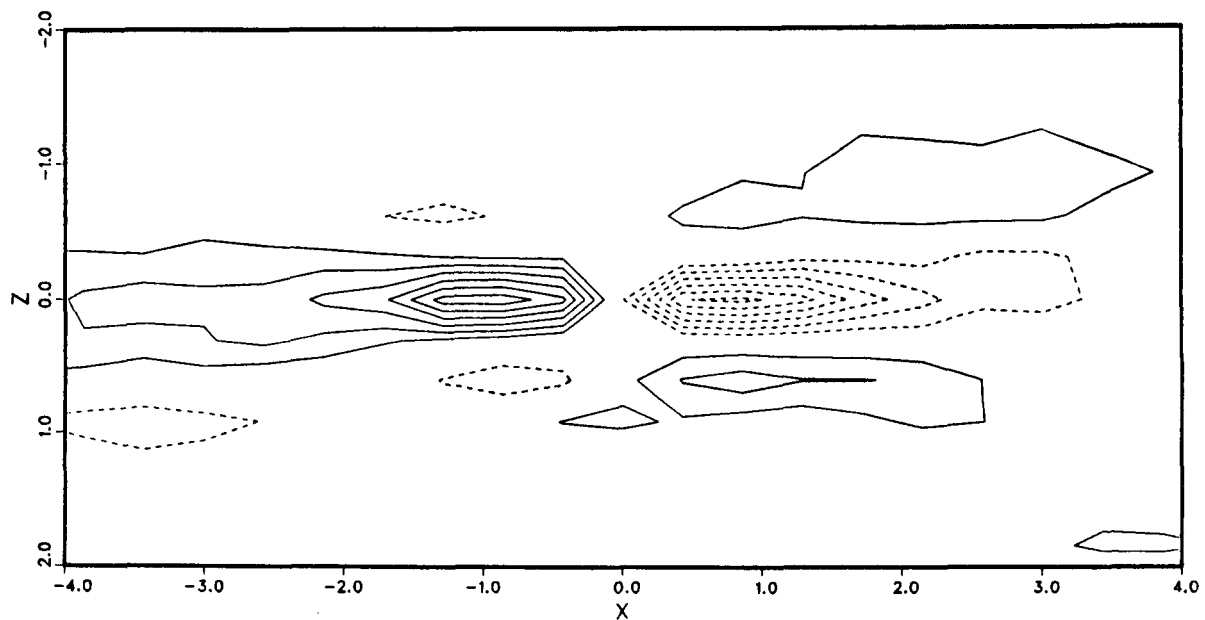


FIGURE 8. Contours of conditionally averaged velocities: a) streamwise velocity in the  $xy$ -plane along the center of the shear layer; b) normal velocity in the  $xy$ -plane; c) streamwise velocity in the  $zz$ -plane at  $y = 0.22$ . Note that  $y$  is measured from the bottom of the channel, and the tick marks denote 70 wall units.

The results from the wave area were somewhat different. The fluctuating components were larger, and the profile of rms fluctuations indicated the typical shape of the least stable T-S wave profile. The Reynolds stress was much higher in the wave area than inside the turbulent part, indicating high turbulence production in the

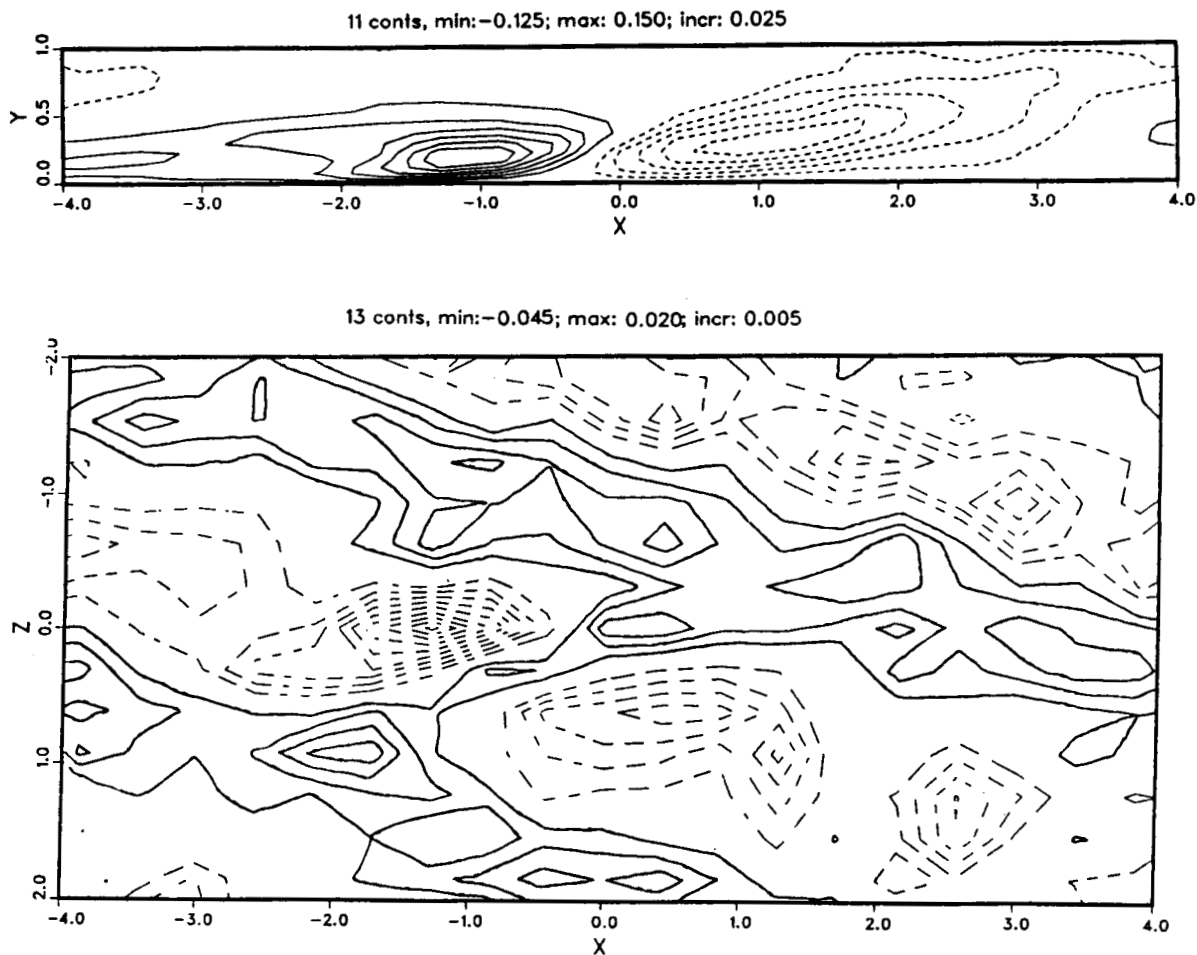


FIGURE 9. Contours of conditionally averaged velocities: a) streamwise velocity in the  $xy$ -plane; b) normal velocity in the  $xy$ -plane; c) streamwise velocity in the  $zz$ -plane at  $y = 0.22$ .

wave area. This is a property in common to T-S wave transition, and has been observed both in experiments (Klebanoff et al., 1962) and simulation (Gilbert, 1988). The appearance of shear layers in the wave area is also typical of the T-S wave transition. The small-scale structure in the cross wave direction captured by the conditional averaging procedure is typical of secondary instability associated with T-S wave breakdown. Thus the transition from laminar to turbulent flow seems to follow a similar pattern in the wingtip area of the spot as in the 2D vibrating ribbon experiments.

#### Acknowledgment

We would like to thank Arne Johansson for many fruitful discussions.

## REFERENCES

BREUER, K. S. 1988 The development of a localized disturbance in a boundary layer. FDRL Report No. 88-1, Dept. Aero. & Astro., MIT

CHAMBERS, F. W. & THOMAS, A.S.W. 1983 Turbulent spots, wave packets and growth.. *Phys. Fluids.* **26**, 1160.

GILBERT, N. 1988 Numerische simulation der transition von der laminaren in die turbulente kanalstromung. Ph.D. Thesis, Fakultat fur Maschinenbau der Universitat Karlsruhe.

GUSTAVSSON, L. H. 1978 On the evolution of disturbances in boundary layer flows.. Ph.D. Thesis, Dept. of Mech., R. Inst. Tech., Stockholm, Sweden.

HENNINGSON, D. S. 1988 The inviscid initial value problem for a piecewise linear mean flow.. *Stud. Appl. Math.* **78**, 31.

HENNINGSON, D. S. 1988 On the spreading mechanism of a turbulent spot in plane Poiseuille flow. 2nd Europ. Turb. Conf., Berlin.

HENNINGSON, D. S. & ALFREDSSON, P. H. 1987 The wave structure of turbulent spots in plane Poiseuille flow. *J. Fluid Mech.* **178**, 405.

HENNINGSON, D. S., SPALART, P. R. & J. KIM 1987 Numerical simulations of turbulent spots in plane Poiseuille and boundary layer flows. *Phys. Fluids.* **30**, 2914.

JOHANSSON, A. V., ALFREDSSON, P. H. & J. KIM 1987 Shear-layer structure in near-wall turbulence. Proc. of CTR summer program, NASA Ames - Stanford, 237.

JOHANSSON, A. V., HER, J. Y. & J.H. HARITONIDIS 1987 On the generation of high-amplitude wall-pressure peaks in turbulent boundary layers and spots. *J. Fluid Mech.* **175**, 119.

KLEBANOFF, P. S., TIDSTROM, K. D. & SARGENT, L. M. 1962 The three dimensional nature of boundary layer transition. *J. Fluid Mech.* **12**, 1.

KIM, J. 1985 Turbulence structure associated with the bursting event. *Phys. Fluids.* **28**, 52.

KIM, J., MOIN, P. & MOSER, R. D. 1987 Turbulence statistics in fully developed channel flow at low Reynolds number. *J. Fluid Mech.* **177**. **133**.

KLINGMANN, B., ALFREDSSON, P. H. & HENNINGSON, D. S. 1988 An experimental study of the velocity field of turbulent spots in plane Poiseuille flow. 2nd Europ. Turb. Conf., Berlin.

LANDAHL, M. T. 1975 Wave breakdown and turbulence. *SIAM J. Appl. Math.* **28**, 735.

NISHIOKA, M., IIDA, S. & ICHIKAWA, Y. 1976 An experimental investigation of the stability of plane Poiseuille flow.. *J. Fluid Mech.* **72**, 731.

RILEY, J. J. & GAD-EL-HAK, M. 1985 The dynamics of turbulent spots. *Frontiers of Fluid Mechanics* (Eds. Davis & Lumley), Springer, 123.

WYGNANSKI, I., SOKOLOV, N. & D. FRIEDMAN 1976 On a turbulent spot in a laminar boundary layer. *J. Fluid Mech.* **78**, 785.